IEEE Access
Multidisciplinary ⋮ Rapid Review ⋮ Open Access Journal

Received May 13, 2020, accepted June 7, 2020, date of publication June 17, 2020, date of current version July 7, 2020.

Digital Object Identifier 10.1109/ACCESS.2020.3002954

Experimental Investigation of Operability in Six-DOF Gesture-Based Operation Using a Lower Limb and Comparison With That in an Upper Limb

MASAHARU KOMORI, (Member, IEEE), TATSURO TERAKAWA, AND IKKO YASUDA
Department of Mechanical Engineering and Science, Kyoto University, Kyoto 6158540, Japan

Corresponding author: Tatsuro Terakawa (terakawa@me.kyoto-u.ac.jp)

This work was supported by the JSPS KAKENHI under Grant 19H02053.

ABSTRACT To operate robots and machines intuitively, interfaces using body motion have recently been investigated. However, compared to the upper limbs, the lower limb operation has not been fully explored. In the present paper, we conducted an experiment involving the six-degree-of-freedom operation of an imaginary object with a lower or upper limb gesture using a virtual-space-based evaluation system. We analyzed the motions of the upper and lower limbs in the operation and discussed the difference between their characteristics. The experimental results showed that the operability of the lower limb was lower than that of the upper limb in terms of time by approximately 79%, accuracy by approximately 109%, subjective evaluation by approximately 39%, and frequency of ON/OFF switching by approximately 82%. We analyzed the results in detail by defining the operational ideality and roughness based on fuzzy estimation. The results clarified that the ideality of the lower limb operation was lower than that of the upper limb by approximately 20–25% and that the ideality was lower in the posture operation than in the position operation by approximately 7–13%. Evaluation of the macro-approaching motions using the roughness index showed that the moving distance, rotating angle, and rotating velocity for a single motion were all smaller in the lower limb operation than in the upper limb operation by approximately 18%, 44%, and 33%, respectively. Consequently, there was the main difference between the upper and lower limbs in the posture operation.

INDEX TERMS Gesture, lower limb, operability, six degrees of freedom, upper limb.

I. INTRODUCTION

Interfaces, through which operators communicate with machines, have an enormous effect on operability in real-time operation, such as teleoperation of machines or teaching tasks of robots. Conventional interfaces often use buttons or levers for manipulation. However, this kind of operating method requires some skill for operation as intended. In order for even novices to experience intuitive operation, the operating method in which the body motion of the operator is measured and converted into the input to the machine is proposed [1]–[7]. In these methods, the robot is controlled to trace the body motion as it is. In addition, the methods by which to command rotation in an arbitrary direction by recognizing hand shapes [8], and to manipulate a robot arm by measuring the three-dimensional (3D) motion of the palm and fingers [9] have been also investigated.

In these gesture-based methods, the upper limbs, including both hands and arms, are mainly selected as measurement objects. Since the upper limbs of human beings are often used for manipulation and operation in daily life, the idea of commanding a similar motion in machines appears natural and easy to accept. In contrast, the lower limbs, including the feet and legs, are basically used to support body weight or walking, but seldom for complicated operations. On the other hand, the lower limb has a skeletal system similar to that of the upper limbs [10], which suggests that an appropriate understanding of its motion characteristics leads to the development of a novel interface for the lower limbs. In fact, the authors and other researchers in a human-computer interface field have developed operating methods using the foot [11]–[16]. However, previous studies focused primarily on proposing operational devices, rather than quantitatively

The associate editor coordinating the review of this manuscript and approving it for publication was Kang Li.

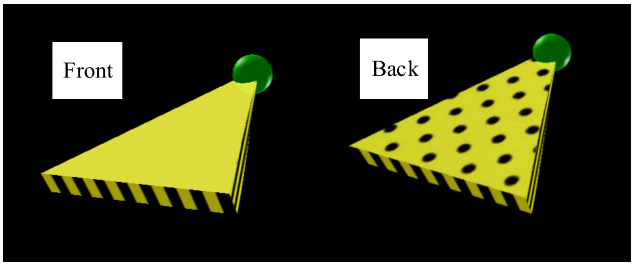

FIGURE 1. Imaginary operated object (IOO) used in the proposed virtual-space-based evaluation system.

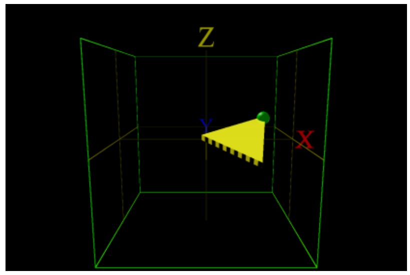

FIGURE 2. Virtual operation space and IOO displayed to operator.

investigating the effectiveness of operation by the lower limb [17]–[19]. This is particularly important in both academic and industrial fields, but the advantages of lower limb operation compared to upper limb operation have not yet been clarified. As for the spatial operation of machines or robots by using lower limbs [19]–[24], no researches have targeted free manipulation with six-DOF in terms of position and posture simultaneously, although the handling of a rigid body in 3D space often requires free six-DOF operation at the same time.

Therefore, the present paper attempts to evaluate the operability in six-DOF gesture-based operation using the lower limb and to compare the results with those for the upper limb. A virtual-space-based evaluation system is constructed, and an experiment in which tasks are assigned to operate an imaginary object with the lower or upper limb gestures is conducted, through which their operability is quantitatively evaluated. The operation on the way to the target position and posture are analyzed based on the fuzzy estimation method in order to clarify the differences in operational characteristics between the lower and upper limbs.

II. EVALUATION SYSTEM FOR LOWER AND UPPER LIMB GESTURE-BASED OPERATION

This section describes the system used in the present research to evaluate the position and posture operation of an object with upper and lower limb motions.

A. VIRTUAL-SPACE-BASED EVALUATION SYSTEM

In the proposed system, we adopt the operation style in which an imaginary operated object (IOO) placed in virtual space is operated, instead of an actual robot or machine placed in real space [25]–[28]. This system was selected considering the difficulty in displaying the target position and posture in real space and the constraint or danger with respect to the movable range and moving performance of an actual machine. The IOO presented to the operator is shown in Fig. 1. The IOO should be a simple object with minimal features with respect to position and posture. Here, a yellow triangle with a green sphere fixed on the tip is used. The green sphere shows the representative point for the position of the IOO, and the orientation of the triangle represents the posture of the IOO. In order to distinguish each surface, the back surface has a pattern of dots, whereas the bottom and side surfaces have stripes with different directions. The virtual operation space is indicated by a skeleton cube with green edges as the operable range of the IOO. As shown in Fig. 2, the operator sees the virtual operation space and the IOO from a fixed viewpoint obliquely from above.

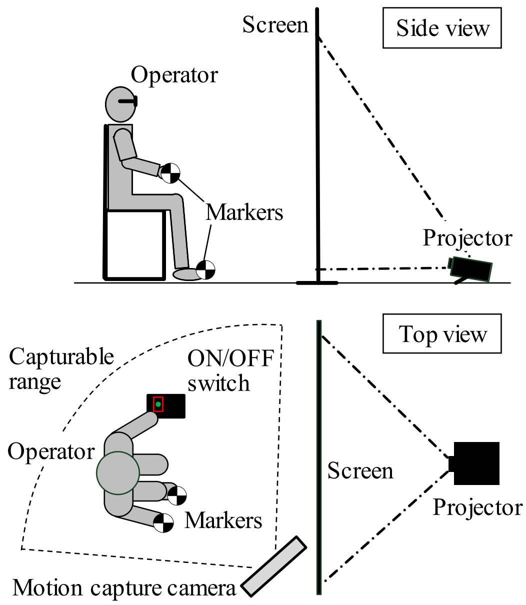

FIGURE 3. Arrangement of experimental setup and operator for the proposed evaluation system.

The setup of the evaluation system is shown in Fig. 3. The virtual operation space and the IOO are drawn by computer software for 3D space indication (SOLIDRAY Ltd., Omega Space) and are projected onto a screen with a specialized projector. The operator wears active shutter glasses (NVIDIA Corporation, 3D VISION2) that enable the operator to see the virtual operation space and the IOO stereoscopically. The position and posture of the IOO are calculated by a PC. The projector, screen, and operator are arranged such that the center of the screen faces the body of the operator when the operator looks directly ahead. The distance between the operator and the screen is about 1.5 m.

B. UPPER/LOWER LIMB GESTURE-BASED OPERATING METHOD

There are two types of methods for operating the position and posture of the IOO by measuring the gestures of body parts. The first is to recognize patterned upper or lower limb movements and generate corresponding commands

(a) (b)

FIGURE 4. Markers to measure the position and posture by a motion capture camera. (a) Marker equipment mounted on foot. (b) Marker equipment mounted on hand.

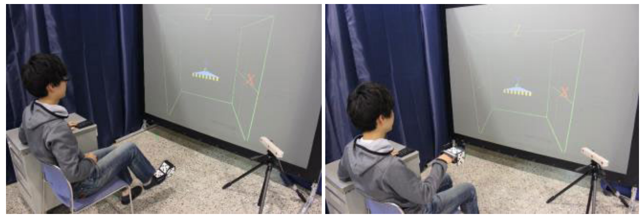

(a) (b)

FIGURE 5. Experimental scenes for the proposed evaluation system. (a) Lower limb gesture-based operating method. (b) Upper limb gesture-based operating method.

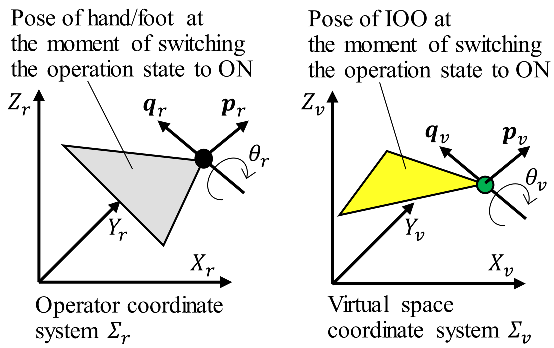

FIGURE 6. Hand/foot motion measured in the real world and the IOO motion in the virtual operation space.

[29]–[32], and the other is the master-slave method, in which the IOO performs the same movement as the upper/lower limb [33]–[36]. The present study uses the master-slave method. The six-DOF motion of the position and posture of the IOO is operated by measuring the position and posture of the hand or foot with a contactless sensor and sending the IOO a command to perform the same motion. In addition to the upper/lower limb gesture, we introduce ON/OFF switching of the operation. The ON state is the state in which the motion of the hand/foot is input to the IOO, which is used to operate the IOO. The OFF state is the state in which the motion of the hand/foot is not input to the IOO, which is used to reset the upper/lower limb state. First, the operator operates the IOO in the ON state. When the upper/lower limb approaches the limit of the movable range and the posture becomes difficult to maintain during the operation, the state is switched to the OFF state. Moreover, the operator returns his/her hand to a comfortable pose and then switches the state ON again in order to resume the operation. By repeating the above process, it is possible to operate the IOO to the arbitrary target position and posture without regard to the movable range of the upper/lower limb. For operating the position, the displacement of the coordinate of the hand/foot is added to that of the IOO. As a result, the IOO moves in the same direction as the hand/foot. With respect to the posture operation, the postural displacement of the hand/foot is input to the IOO so that the rotation axis vector and the rotation angle of the hand/foot as seen from the operator agree with those of the IOO as seen through the screen.

The position and posture of the marker mounted on the hand/foot of the operator are measured to estimate the position and posture of the hand/foot. As shown in Fig. 4, several markers are fixed on each of the hand and foot via equipment in order to reduce dead angles. The measurement is conducted using a camera-based real-time motion-capture system (Claron Technology Inc., Micron Tracker H3-60). The position and posture of the marker are sent to a PC. The displacement is then calculated, and the command is input to the IOO. Fig. 5 shows the actual experimental scene, where the arrangement of the camera, marker, and operator is basically the same as Fig. 3. The operator can switch the ON/OFF state using an input device (ON/OFF Switch). The device has a button, which brings the system into the ON state while the button is pushed and into the OFF state while the button is released. The maker is mounted on the right hand or right foot of the operator. The ON/OFF switch is operated by the left hand.

The motion capture camera provides the current positions and rotational matrices of the markers relative to the reference coordinate system. The IOO motion is calculated from the measured hand/foot motion in the following way. First, the coordinate system Σ_r fixed to the operator and Σ_v fixed to the virtual operation space are defined as shown in Fig. 6. In Σ_r, the X_r, Y_r, and Z_r axes point to the right, forward, and upward of the operator, respectively. In Σ_v, the X_v, Y_v, and Z_v axes point to the right, forward, and upward of the virtual operation space, respectively, seen from the operator. As for the position operation, we set the displacement of the hand/foot from the position at the moment when the operation state is switched to ON as $\boldsymbol{p}_r$. At this time, the displacement input to the IOO $\boldsymbol{p}_v$ is given as

$$\boldsymbol{p}_v = c\boldsymbol{p}_r \tag{1}$$

where c is a scale factor. This means that the IOO moves in the same direction in Σ_v as the hand/foot moves in Σ_r. With respect to the posture operation, we assume that the hand/foot rotates around a vector $\boldsymbol{q}_r$ at an angle θ_r. Then, the quaternion corresponding to this rotation is represented as follows:

$$\tilde{q}_r = \cos\frac{\theta_r}{2} + \boldsymbol{q}_r \sin\frac{\theta_r}{2}. \tag{2}$$

The IOO rotates in the same way as the hand/foot. Namely,

$$\tilde{q}_v = \tilde{q}_r \tag{3}$$

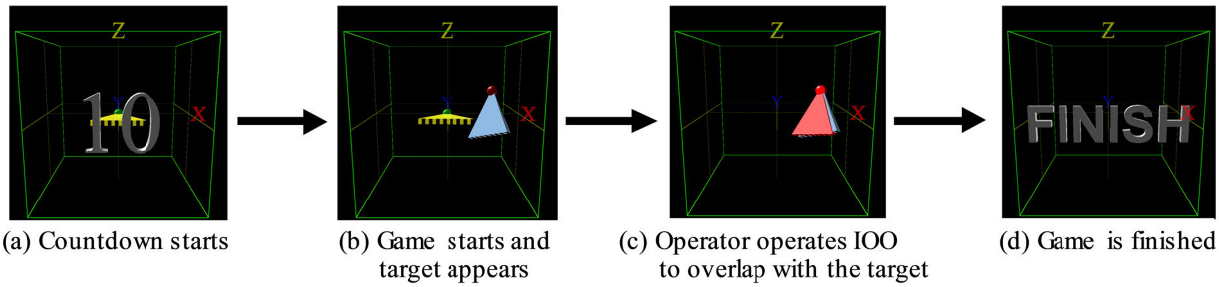

FIGURE 7. Flow of one evaluation game carried out in the proposed evaluation system.

where $\tilde{q}_v$ is a quaternion of the IOO defined in Σ_v. Note that the IOO moves in the virtual operation space just as commanded without any inertial or frictional effect.

III. EXPERIMENTAL EVALUATION OF LOWER LIMB GESTURE-BASED OPERATION AND COMPARISON WITH THE UPPER LIMB

Using the evaluation system proposed in the previous section, an experiment is conducted to evaluate the operating method using the lower limb motion quantitatively and to compare the motion to that using the upper limb.

A. EVALUATION GAME

In the experiment, as shown in Fig. 7, the evaluation game was held such that the targets that had the same shape as the IOO were displayed in the virtual space and the operator operated the IOO to overlap with the target. The target appeared in the virtual operation space at a random position and posture. However, since it was difficult to determine the target posture if the operator could only see its side or bottom surface, such targets were excluded. The movable ranges of the IOO and the target are limited within the cubic operational space with a dimensionless side length of 30, which is equivalent to a cube of 600 mm on each side in real space. In the analyses discussed below, we basically use this dimensionless scale. When the positions of the IOO and the target agree with each other, a sphere fixed to the tip of the triangle changes from green to red in order to indicate agreement to the operator. When the IOO and the target have overlapped completely, the entire IOO is displayed in red, as shown in Fig. 7(c). When this state remains for one second, the target is cleared. The decisions of the position and posture matching are carried out independently, and their criteria are as follows:

1) POSITION MATCHING JUDGMENT

We set the coordinates of the IOO in Σ_a as $\boldsymbol{\xi}_h$ and the coordinates of the target in Σ_a as $\boldsymbol{\xi}_T$. When the condition of $\left\|\boldsymbol{\xi}_h - \boldsymbol{\xi}_T\right\| \leq 1$ is satisfied, the state is determined such that the positions of the IOO and target are in agreement.

2) POSTURE MATCHING JUDGMENT

We set $(\boldsymbol{x}_h\ \boldsymbol{y}_h\ \boldsymbol{z}_h)$ as the rotation matrix of the IOO seen from Σ_a and $(\boldsymbol{x}_T\ \boldsymbol{y}_T\ \boldsymbol{z}_T)$ as the rotation matrix of the target seen from Σ_a. When the condition $\min\left(\langle \boldsymbol{x}_h, \boldsymbol{x}_T\rangle, \langle \boldsymbol{y}_h, \boldsymbol{y}_T\rangle\right) \geq 0.99$ is satisfied, the state is determined such that the positions and postures of the IOO and target coincide. Note that $\langle *, * \rangle$ represents the internal product.

The flow of the game is as follows (Fig. 7):

(a) The IOO is displayed at the center of the operational space, and a 10-second countdown starts.

(b) At the moment when the countdown reaches zero, the target appears.

(c) The operator operates the IOO to overlap with the target.

(d) When the displayed target is cleared, the game ends and FINISH is displayed.

B. EVALUATION INDICES

In the experiment, the clear time required to finish the game, the moving path of the IOO in the game, and the survey given to the test subjects were used as evaluation indices for the operability of the upper/lower gesture-based operation. The operability in tasks is considered to be better when the operated object can move to the target position and posture in a shorter time. It was evaluated based on the game clear time. Moreover, the operability will also be better if the operation contains fewer useless motions. We evaluated it according to the ratio of the path length along which the IOO actually moved to the shortest path length from the initial position to the target position. As this ratio approaches 1, the moving path approaches the optimal path, and the motion is judged to be less useless.

In addition to these objective indices, a questionnaire survey was carried out in order to investigate the subjective evaluation of each operating method. The evaluation item was "whether or not it was easy to manipulate the IOO" and the questionnaire was taken once for each of the upper and lower limb operating methods. Here, the visual analog scale (VAS) method was used for the questionnaire. The questionnaire sheet on which a line with no scale was drawn was given to the subject, and the subject placed a mark on the line at the most suitable point, supposing that the left and right ends of the line indicate "hard to operation" and "easy to operate", respectively. The distance from the left end of the line to the position marked by the subject was converted to a point between 0 and 100, which is used as the evaluation by the subject of the operation method.

C. EXPERIMENTAL PROCEDURE

The test subjects of the experiment were 12 healthy adult men without injury or disability. The average age was 23.6 years, with a standard deviation of 1.30 years. First, it was explained

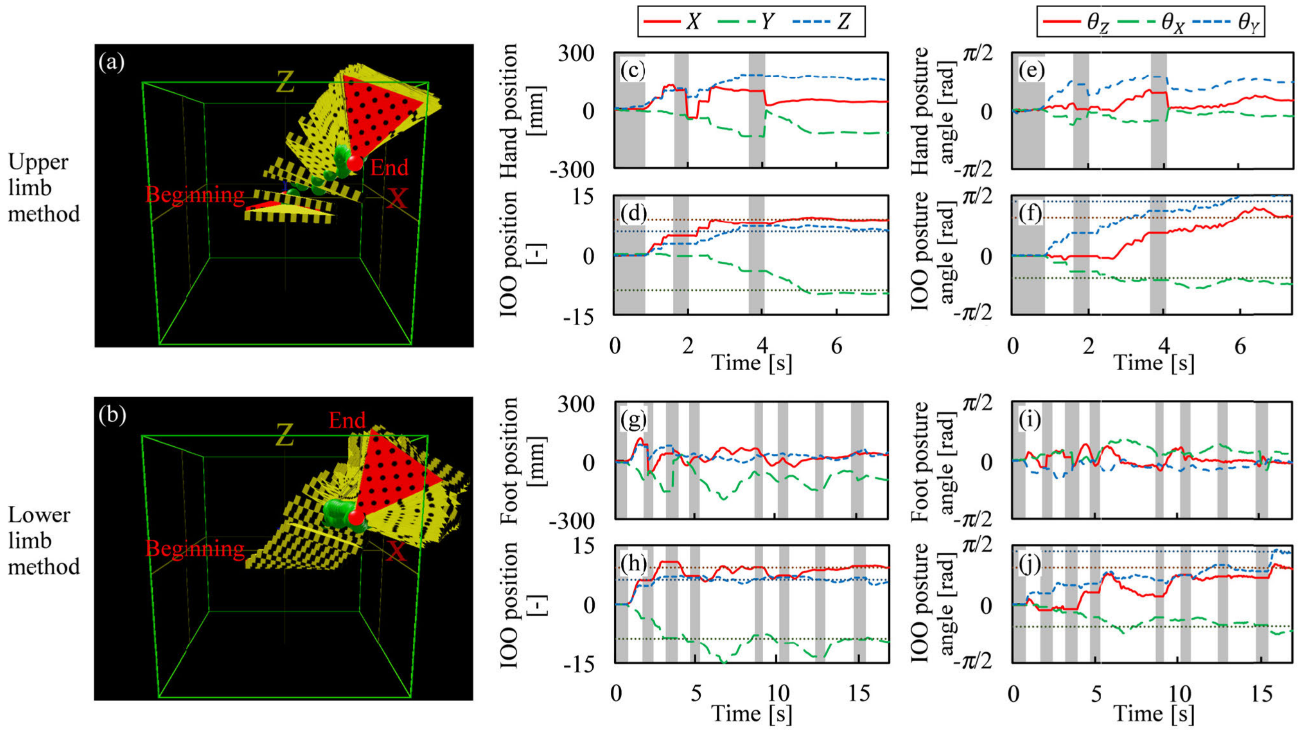

FIGURE 8. Experimental result of IOO and hand/foot motions in an evaluation game for the upper and lower limb operating methods: (a), (b) Actual IOO motion in the virtual operation space. (c)–(j) Time variation of the position and posture angle of the hand/foot and the IOO, where the white and gray areas indicate the ON and OFF state period, respectively, and the dotted lines in the IOO's results indicate the target value of the parameters.

that the displayed IOO was to be operated, and the target indicated the goal position and posture of the IOO. After the upper and lower limb gesture-based operating methods were explained with the demonstration, each subject experienced practice games three times in order to get used to the operation and the game. Before starting the operation, the subject was shown a cubic model with a side length of 300 mm and was instructed to move his hand or foot within the model. The subject was asked to switch the operation state to OFF when his hand or foot was likely to move out of the designated range or when maintaining the pose during operation seemed difficult, and the subject was then asked to switch the operation state to ON after returning his hand/foot to around the center of the range and a comfortable posture. The subject was required to try to clear games as quickly as possible and to move the IOO to the target with the shortest distance. In the experiment, 20 games were carried out for each of the upper/lower limb operating methods, i.e., 40 games in total for each subject. The questionnaire was given when 20 games of each operating method were finished.

In order to prevent the order of the experiments from affecting the results, the experiment of the upper limb method was conducted first for six subjects, and the lower limb method was conducted first for the other six subjects. In addition, games were given in random order for each subject and each operating method from the 20 prepared patterns. This experiment was conducted with the approval of the Ethics Committee, Graduate School of Engineering, Kyoto University.

D. EXPERIMENTAL RESULTS AND DISCUSSIONS

1) TRAJECTORY OF MOTION

Fig. 8 shows a typical example of the measured motion in one evaluation game for one test subject. Fig. 8(a) and (b) illustrates the actual IOO motion in the virtual operation space. The IOO seems to move directly to the target state in the upper limb method [Fig. 8(a)] but indirectly in the lower limb method [Fig. 8(b)]. Fig. 8(c) to (j) shows the trajectories of the position and posture in the hand/foot motion and the IOO motion from beginning to end of the game. Here, the IOO position is represented by the dimensionless scale used in the virtual operating space. The posture angles of the hand/foot and the IOO are represented by the Euler angles of the Z-X-Y system θ_Z, θ_X, and θ_Y. If the IOO moves directly to the target, the trajectory of the hand/foot should increase or decrease monotonously during the ON period. Fig. 8(c) and (e) shows that the trajectories of the hand position and posture satisfy it, respectively, especially for 0.9–1.6 s and 2.1–3.6 s. On the other hand, fluctuations of the trajectory in one ON period lead to the indirect motion of the IOO, which causes ineffective motions. This behavior can be seen in the trajectory of the foot position and posture, e.g., for 5.2–8.6 s in Fig. 8 (g) and (i), respectively. One of the reasons for this result might be the range of motion. In general, the range of motion of the foot is smaller than that of the hand, especially in the pronation/supination motion [37], [38]. Such a limited joint motion makes it difficult to operate the IOO as the operator intended. Another possible factor is subordination between the joints. When abduction/adduction

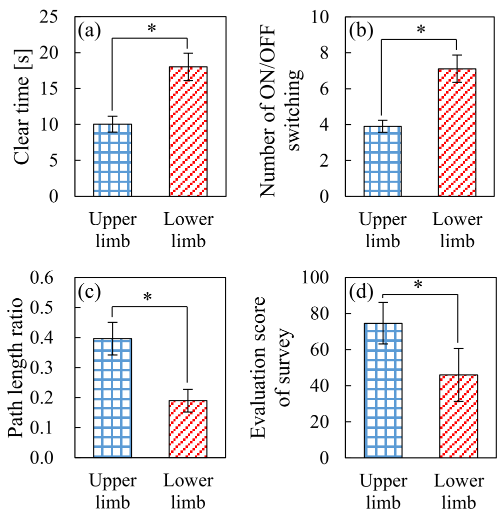

FIGURE 9. **Experimental results (∗: $p < 0.05$). (a) Average clear time for one evaluation game. (b) Average number of ON/OFF switching times in one evaluation game. (c) Average path length ratio between the ideal and actual paths for one evaluation game. (d) Average value of questionnaire survey evaluation.**

or pronation/supination is generated, the foot tends to make the other motion at the same time without regard to the operator's intention [39]. This phenomenon is considered to be involved in the indirect motion of the foot.

2) CLEAR TIME RESULTS

Fig. 9(a) shows the average values and confidence intervals of the clear time per game for all participants. The average clear time of the upper and lower limb methods were 10.0 s and 18.0 s, respectively, between which there was a significant difference at the 5% level of significance according to the Mann-Whitney U test. Comparing the average values, the clear time of the lower limb method is longer than that of the upper limb method by 8.0 s, i.e., approximately 79% in proportion. The standard deviations of the clear time were 2.5 s in the upper limb method and 4.3 s in the lower limb method. Hence, the variation of the clear time became larger in the lower limb method.

The average values and confidence intervals of the number of times the subject switches the ON/OFF state in one game are shown in Fig. 9(b). The average values were 3.9 times and 7.1 times for the upper and lower limb methods, respectively, which is approximately 82% larger for the lower limb method. Comparing Fig. 9(a) and (b), there may be a correlation between the clear time and the number of ON/OFF switching times. In general, the movable range of the foot joint is smaller than that of the hand joint. This suggests that the clear time in the lower limb method became larger because the limited joint range of motion, especially in the posture operation, caused the test subject to input the motion in which the ON/OFF state was switched several times.

3) PATH LENGTH RATIO

Fig. 9(c) shows the average values and confidence intervals of the path length ratio per game for all test subjects. The average values of the path length ratio were 0.40 and 0.19 for the upper and lower limb methods, respectively, between which there was a significant difference at the 5% level of significance according to the U test. Comparing the average values, the result for the lower limb is worse than that for the upper limb by approximately 109%. This result means that the lower limb method causes more useless motions during the operation than the upper limb method. This result agrees with the intuitive recognition that the lower limb is generally unaccustomed to operation and inaccurate with respect to motion, as compared to the upper limb. In addition, ON/OFF switching may affect the results in this experimental condition. Namely, since the motion is disrupted before and after switching the ON/OFF state, the hand or foot can be moved in an unintended direction when resuming the operation. Therefore, it is considered that the lower limb method easily causes the deviation from the shortest path because ON/OFF switching is frequently required.

As shown in Fig. 9(a) through (c), the operability of the lower limb in multi-DOF operation could be evaluated quantitatively and compared to that of the upper limb using the proposed evaluation system.

4) QUESTIONNAIRE RESULTS

The questionnaire result for each operating method is shown in Fig. 9(d). The average score for all test subjects was 74.6 for the upper limb method and 46.0 for the lower limb method. Based on the U test, there was a 5% level of significant difference between these results. A comparison of the average values showed that the subjects felt more difficulty in operating the lower limb method than the upper limb method at a rate of 39%. This result agrees with the results of the objective indices, i.e., the clear time and path length ratio. Thus, it was verified that the proposed system could quantitatively evaluate even a vague index of operability, which is difficult to express in figures.

IV. ANALYSIS OF INDIVIDUAL OPERATION IN THE ON STATE

In the previous section, we evaluated the total time and path from the start to the end of the game to compare the upper and lower limbs. However, the operation in a game actually contains multiple motions resulting from ON/OFF switching, so that each motion in an ON state may also have differences between the characteristics of the upper and lower limbs. Here, we define an ON period as the time of a single ON state between the previous and next OFF states and focus on each motion to move and rotate the IOO from one state to another during an ON period. In terms of the hand and foot motion measured in the experiment of Section III, the ideality of the motion during each ON period is evaluated, and the moving distance/velocity and rotating angle/velocity are analyzed. The present paper uses fuzzy estimation for these analyses [40]–[43].

A. IDEALITY EVALUATION OF OPERATION

First, whether or not the IOO approaches the target during the operation in each ON period is evaluated. We explain the

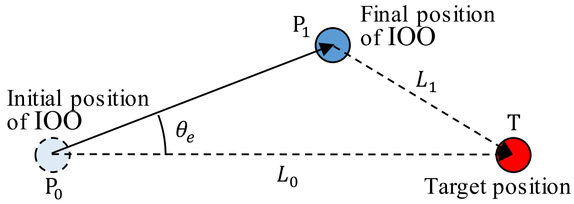

FIGURE 10. Ideality model for a movement of IOO during single operation in an ON period.

definition of the ideality for the position operation. As shown in Fig. 10, the initial and final positions of the IOO in the ON state are set as P_0 and P_1, respectively, and the target position is set as T. Considering that the motion is ideal when P_1 and T coincide, the method by which to determine the ideality is discussed when P_1 is different from T. For the estimation, two fuzzy sets A and B are prepared.

A : The difference between the ideal and actual directions in which the IOO moves is small.

B : The distance between the IOO and the target is shortened.

According to the combination of A and B, the following four rules are determined:

Rule 1: If A and B, then the ideality of the position operation is I_1.

Rule 2: If $\overline{A}$ and B, then the ideality of the position operation is I_2.

Rule 3: If A and $\overline{B}$, then the ideality of the position operation is I_3.

Rule 4: If $\overline{A}$ and $\overline{B}$, then the ideality of the position operation is I_4.

When the moving direction and distance of the IOO toward the target in the single operation are given, we define the membership functions for $A, \overline{A}, B$, and $\overline{B}$, which represent how the parameters satisfy each fuzzy set, as follows:

$$\mu_A(\theta_e) = 1 - \frac{\theta_e}{\pi} \quad (0 \leq \theta_e \leq \pi) \tag{4}$$

$$\mu_{\overline{A}}(\theta_e) = 1 - \mu_A(\theta_e) = \frac{\theta_e}{\pi} \quad (0 \leq \theta_e \leq \pi) \tag{5}$$

$$\mu_B\left(\frac{L_1}{L_0}\right) = \begin{cases} 1 - \frac{L_1}{L_0} \left(0 \leq \frac{L_1}{L_0} < 1\right) \\ 0 \left(1 \leq \frac{L_1}{L_0}\right) \end{cases} \tag{6}$$

$$\mu_{\overline{B}}\left(\frac{L_1}{L_0}\right) = 1 - \mu_B\left(\frac{L_1}{L_0}\right) = \begin{cases} \frac{L_1}{L_0} \left(0 \leq \frac{L_1}{L_0} < 1\right) \\ 1 \left(1 \leq \frac{L_1}{L_0}\right) \end{cases} \tag{7}$$

where θ_e (radian) indicates the angle between $\overrightarrow{P_0P_1}$ and $\overrightarrow{P_0T}$, L_0 and L_1 (dimensionless) indicate the lengths of $\overrightarrow{P_0T}$ and $\overrightarrow{P_1T}$, respectively, and μ_A, $\mu_{\overline{A}}$, μ_B, and $\mu_{\overline{B}}$ are the membership functions for A, $\overline{A}$, B, and $\overline{B}$, respectively. As for A, the motion is considered to be ideal when the difference in the moving direction of the IOO from the ideal direction is small. Then, we designed μ_A as a function of θ_e that decreases in proportion to θ_e. With respect to B, the motion is judged to be ideal as the IOO approaches the target. Then, μ_B is designed as a function of L_0/L_1 that decreases in proportion for $0 \leq L_0/L_1 < 1$ and becomes constant $\mu_B = 0$ for $L_0/L_1 \geq 1$.

Next, we conduct defuzzification according to Rules 1 through 4 by Sugeno's method. When the goodness of fit for Rule 1 is set as C_1, it is defined by the following equation.

$$C_1 = \min(\mu_A, \mu_B) \tag{8}$$

The same is true for the goodness of fit of Rules 2 through 4 C_2, C_3, and C_4. Namely,

$$C_2 = \min(\mu_{\overline{A}}, \mu_B) \tag{9}$$

$$C_3 = \min(\mu_A, \mu_{\overline{B}}) \tag{10}$$

$$C_4 = \min(\mu_{\overline{A}}, \mu_{\overline{B}}). \tag{11}$$

At this time, the ideality of the operation I_{total} is

$$I_{\text{total}} = \frac{1}{I_{\max}} \frac{\sum_{i=1}^{4} C_i I_i}{\sum_{i=1}^{4} C_i} \tag{12}$$

where $I_{\max} = \max(I_1, I_2, I_3, I_4)$. The term $1/I_{\max}$ in the equation normalizes the total ideality.

The ideality for the posture operation of the IOO is defined in the same manner as the ideality of the position operation. Specifically, points P_0 and P_1 are defined in the posture space instead of the position space, as shown in Fig. 13, and then the ideality is calculated from (4) through (12).

Fig. 11 shows the calculated results of the ideality for the upper and lower limb methods concerning all position and posture operations for all test subjects in the experimental results of Section III. The operation in each ON period contains the position and posture operation, so that the ideality can be calculated. The value of the ideality for each Rule is given as $I_1 = 3$, $I_2 = 2$, $I_3 = 1$, and $I_4 = 0$. We determined these values by four-grade evaluation considering that if Rules 1 through 4 are satisfied, the ideality can be high in this order. In the figure, the horizontal axis indicates the ideality of the position operation, and the vertical axis indicates the ideality of the posture operation. According to the Mann-Whitney U test, the ideality of each operating method has a significant difference at the 5% level between the median values of the two groups in both the position and posture operation. The average values of the ideality for the position and posture operation of the upper and lower limbs are shown in Fig. 12. The average ideality of the lower limb is less than that of the upper limb by approximately 20% and 25% in the posture and position operations, respectively. This is also found in Fig. 11, where the density of the distribution is high in the upper right region for the upper limb method (a) and in the lower left region for the lower limb method (b). Compared to the position operation, the ideality of the posture operation is lower in both the upper and lower limbs by approximately 7% and 13%, respectively. This result suggests that the posture operation is more difficult than the

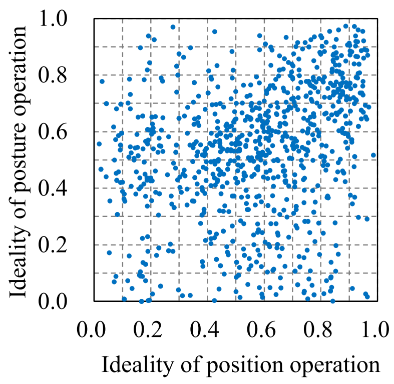

(a) Upper limb gesture-based operating method

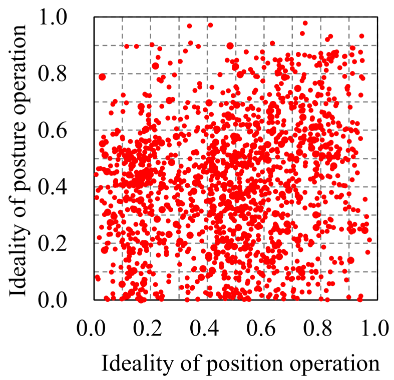

(b) Lower limb gesture-based operating method

FIGURE 11. Evaluation result of operational ideality for all movements observed in the experiment.

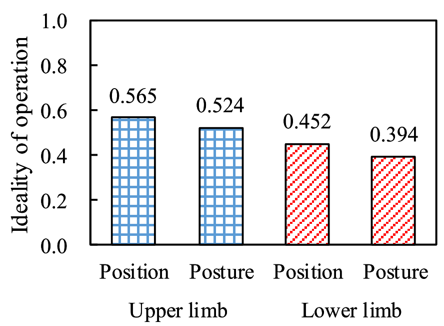

FIGURE 12. Average values of operational ideality shown in Fig. 14.

position operation for both the upper and lower limbs, which is analyzed in detail later.

B. ANALYSIS OF POSITION AND POSTURE OPERATIONS IN THE MACRO-APPROACHING OPERATION

In this section, the moving distance/velocity and rotating angle/velocity of the position and posture operation in each ON period are analyzed and compared between the upper and lower limbs. The task of overlapping the IOO with the target, which was assigned in the experiment, is considered to be classified roughly into two steps. One step is to bring the IOO toward the target roughly and quickly (macro-approaching operation), and the other step is to adjust the IOO to the target carefully. It is expected that the motion characteristics are quite different between these two steps, e.g., the moving distance/velocity and rotating angle/velocity may be larger in the former than in the latter. Therefore, it is difficult to evaluate the displacement or velocity appropriately as long as the former and latter are mingled. As such, we distinguish the macro-approaching operation from the adjustment and evaluate these steps with a focus on the former. Since there are no clear criteria by which to judge whether each operation belongs to the former or latter step, fuzzy estimation is introduced. We define the parameter of roughness, which indicates the degree of the macro-approaching operation, and then evaluate the roughness of each operation based on fuzzy estimation.

The roughness of the position operation is estimated in the following process. First, two fuzzy sets are picked.

C : The moving distance of the IOO is large.

D : The moving velocity of the IOO is large.

According to the combination of C and D, the following four rules are determined

Rule 5: If $C \cap D$, i.e., the moving distance is large and the moving velocity is large, then the roughness of the operation is R_5.

Rule 6: If $C \cap \overline{D}$, i.e., the moving distance is large and the moving velocity is small, then the roughness of the operation is R_6.

Rule 7: If $\overline{C} \cap D$, i.e., the moving distance is small and the moving velocity is large, then the roughness of the operation is R_7.

Rule 8: If $\overline{C} \cap \overline{D}$, i.e., the moving distance is small and the moving velocity is small, then the roughness of the operation is R_8.

Here, assuming that the moving distance, L_p (dimensionless), and moving velocity, V_p [s^{-1}], of the IOO are given, the membership function for each fuzzy set is defined as follows:

$$\mu_C(L_p) = \begin{cases} \frac{L_p}{15} \ (0 \le L_p < 15) \\ 1 \ (15 \le L_p) \end{cases} \quad (13)$$

$$\mu_{\overline{C}}(L_p) = 1 - \mu_C(L_p) = \begin{cases} \frac{1 - L_p}{15} \ (0 \le L_p < 15) \\ 0 \ (15 \le L_p) \end{cases} \quad (14)$$

$$\mu_D(V_p) = \begin{cases} \frac{V_p}{7.5} \ (0 \le V_p < 7.5) \\ 1 \ (7.5 \le V_p) \end{cases} \quad (15)$$

$$\mu_{\overline{D}}(V_p) = 1 - \mu_D(V_p) = \begin{cases} \frac{1 - V_p}{7.5} \ (0 \le V_p < 7.5) \\ 0 \ (7.5 \le V_p) \end{cases} \quad (16)$$

where μ_C, $\mu_{\overline{C}}$, μ_D, and $\mu_{\overline{D}}$ are the membership functions for C, $\overline{C}$, D, and $\overline{D}$, respectively. For C, the roughness is considered to be high when the moving distance of IOO is large. Then, we set μ_C as the function of L_p that increases linearly for $0 \le L_p < 15$ and takes constant $\mu_C = 1$ for $L_p \ge 15$. With respect to D, the roughness is judged to be high as the moving velocity is large. Then, we designed μ_D as a function of V_p that increases linearly for $0 \leq V_p < 7.5$ and becomes constant $\mu_D = 1$ for $V_p \geq 7.5$. The value of $L_p = 15$, which corresponds to 300 mm in the real world, is determined based on the side length of the cubic model shown to the subject in the experiment. The value of $V_p = 7.5$ is set according to the average value of the maximum moving velocity extracted from the data satisfying $L_p \geq 15$.

Next, defuzzification is carried out according to Rules 5 through 8. The goodness of fit for Rule 5 is given as

$$C_5 = \min(\mu_{\mathrm{C}}, \mu_{\mathrm{D}}). \tag{17}$$

Those for Rules 6 through 8, i.e., C_6, C_7, and C_8, are similar.

$$C_6 = \min(\mu_{\mathrm{C}}, \mu_{\overline{D}}) \tag{18}$$
$$C_7 = \min(\mu_{\overline{C}}, \mu_{\mathrm{D}}) \tag{19}$$
$$C_8 = \min(\mu_{\overline{C}}, \mu_{\overline{D}}) \tag{20}$$

At this time, the roughness of the operation R_{total} is

$$R_{\mathrm{total}} = \frac{1}{R_{\max}} \frac{\sum_{i=5}^{8} C_i R_i}{\sum_{i=5}^{8} C_i} \tag{21}$$

where $R_{\max} = \max(R_5, R_6, R_7, R_8)$.

Concerning the roughness of the posture operation, assuming that the rotating angle of the IOO, Θ_p (radian), and the rotating velocity, Ω_p [s^{-1}], are given, the membership functions for the fuzzy sets of ''the rotating angle is large'' and ''the rotating velocity is large'' are defined as

$$\mu(\Theta_p) = \frac{\Theta_p}{\pi}\left(0 \leq \Theta_p \leq \pi\right) \tag{22}$$

$$\mu(\Omega_p) = \begin{cases} \frac{2\Omega_p}{\pi}\left(0 \leq \Omega_p < \frac{\pi}{2}\right) \\ 1\left(\frac{\pi}{2} \leq \Omega_p\right), \end{cases} \tag{23}$$

respectively. The following calculation method is the same as that of the roughness for the moving distance and velocity.

Fig. 13 shows the calculation results for the average moving distance/velocity and rotating angle/velocity weighted by multiplying the roughness defined above. The value of the roughness for each Rule is given as $R_5 = 2$, $R_6 = 1$, $R_7 = 1$, and $R_8 = 0$. These values are determined in the way similar to the ideality in the previous section, except that three-grade evaluation is used because the roughness for Rules 6 and 7 is considered to be the same degree. The graphs show that all indices of the lower limb method are smaller than those of the upper limb method. Moreover, there was a 5% level significant difference in the moving distance, rotating angle, and rotating velocity according to the U test.

This result means that the moving distance or rotating angle during a single operation is smaller in the lower limb than in the upper limb, which agrees with the above-mentioned result that the lower limb requires multiple operations by switching the ON/OFF state many times, as shown in Fig. 9(b).

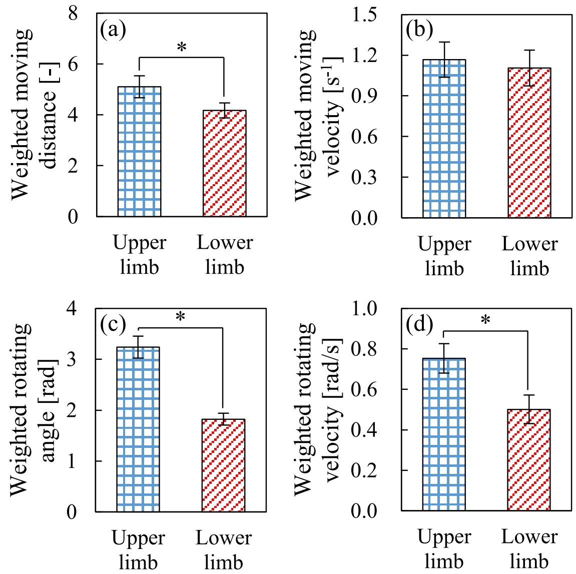

FIGURE 13. Average values of (a) moving distance, (b) moving velocity, (c) rotating angle, and (d) rotating velocity per single operation in an ON period weighed with operational roughness for the movements observed in the experiment (*: $p < 0.05$).

With respect to the moving distance, although both hand and foot could move around the entire range of the 300 mm cube that was presented to the test subject as the standard movable range in the experiment, there was a gap in the moving distance of a single operation, as shown in Fig. 13(a). The rotating angle of the lower limb became smaller than that of the upper limb, likely because the movable range of the foot joint is smaller than that of the hand joint, both of which strongly contribute to the posture change. The reason why the rotating velocity of the lower limb became smaller than that of the upper limb is considered to be the same. In contrast, the moving velocity was not significantly different between the upper and lower limbs.

Next, the position and posture operation are compared. In the position operation, the difference between the upper and lower limbs was relatively small. The moving distance and velocity of the lower limb were approximately 82% and 95% of that of the upper limb. The difference between the upper and lower limbs was relatively large in the posture operation. The rotating angle and velocity of the lower limb were approximately 56% and 67%, as compared to the upper limb. Therefore, it was clarified that the lower limb had a weakness, especially in the posture operation, compared to the upper limb. This might be because the movable range of the foot joint in the lower limb is smaller than that of the hand joint in the upper limb, as mentioned above. This result suggests that the difficulty in the posture operation should be taken into consideration in the design of the interface for the lower limb operation with superb operability.

V. CONCLUSION

Interfaces for the intuitive operation that use the body motion have recently attracted attention. Such interfaces usually use the upper limbs, so that using the lower limb motion may lead to a novel interface. In the present study, in order to clarify the operability of the lower limb motion in multi-DOF operation or how different this operability is from that of the upper limb, we conducted an experiment of operating an IOO with the lower or upper limb gesture using a virtual-space-based evaluation system. We analyzed the motions of the lower and upper limbs in the operation based on fuzzy estimation and discussed the difference between their characteristics. Consequently, we obtained the following results:

1) In order to evaluate the characteristics in the multi-DOF operation of the lower and upper limbs quantitatively, the evaluation system by operating the IOO in virtual space was constructed. An experiment using the proposed evaluation system verified that the upper and lower limb operating methods could be quantitatively evaluated and compared.
2) The experimental results showed that the operational time was longer by 79%, the accuracy in the moving path was worse by 113%, the operability evaluation by the questionnaire was lower by 38%, and the number of ON/OFF switching times was larger by 82% in the lower limb operation, as compared to the upper limb.
3) Focusing on the operation in a single ON period while moving and rotating the object to a target position and posture, a method by which to evaluate the ideality of the position and posture operation quantitatively was proposed using fuzzy estimation. The results clarified that the ideality of the lower limb operation was lower than that of the upper limb by 20–25%. Moreover, the ideality was indicated to be approximately 13% lower in the posture operation than in the position operation.
4) Assuming that the operation to move the object to the target was classified into the macro-approaching operation and the adjustment, its index was defined as the operational roughness based on fuzzy estimation. As a result of evaluating the motions in the macro-approaching operation using the roughness index, the moving distance, rotating angle, and rotating velocity per single motion were all clarified to be smaller in the lower limb operation than in the upper limb operation.
5) The difference between the upper and lower limbs was relatively small in the position operation, but was large in the posture operation, in which the rotating angle and velocity per one motion in the lower limb operation were approximately 54% and 65% of those in the upper limb operation. The lower limb was revealed to have a weakness in the posture operation as compared to the upper limb.

The present study clarified the fundamental difference between the operability of the upper and lower limbs in the free six-DOF manipulation. The future work will handle more detailed experiments of the joint motions with independent DOF or more practical operating method by introducing the aspect of haptics [44]. It will also be interesting to bring new evaluation indices such as jerk. These results will contribute to the development and design of interfaces.

REFERENCES

[1] V. S. Rao and C. Mahanta, "Gesture based robot control," in *Proc. 4th Int. Conf. Intell. Sens. Inf. Process.*, Warsaw, Poland, Dec. 2006, pp. 407–413.
[2] A. Jackowski, M. Gebhard, and A. Graser, "A novel head gesture based interface for hands-free control of a robot," in *Proc. IEEE Int. Symp. Med. Meas. Appl. (MeMeA)*, Benevento, Italy, May 2016, pp. 1–6.
[3] M. T. Wolf, C. Assad, M. T. Vernacchia, J. Fromm, and H. L. Jethani, "Gesture-based robot control with variable autonomy from the JPL BioSleeve," in *Proc. IEEE Int. Conf. Robot. Autom.*, Karlsruhe, Germany, May 2013, pp. 1160–1165.
[4] T. Grzejszczak, A. Legowski, and M. Niezabitowski, "Application of hand detection algorithm in robot control," in *Proc. 17th Int. Carpathian Control Conf. (ICCC)*, Tatranska Lomnica, Slovakia, May 2016, pp. 222–225.
[5] P. Moore, A. A. Kist, A. Maiti, and A. D. Maxwell, "Work in progress: Remote experiment control through gesture recognition," in *Proc. 13th Int. Conf. Remote Eng. Virtual Instrum. (REV)*, Madrid, Spain, Feb. 2016, pp. 377–379.
[6] M. Komori, T. Uchida, K. Kobayashi, and T. Tashiro, "Operating method of three-dimensional positioning device using moving characteristics of human arm," *J. Adv. Mech. Des., Syst., Manuf.*, vol. 12, no. 1, 2018, Art. no. JAMDSM0009.
[7] M. Komori, K. Kobayashi, and T. Tashiro, "Method of position command generation by index finger motion to mitigate influence of unintentional finger movements during operation," *Precis. Eng.*, vol. 53, pp. 96–106, Jul. 2018.
[8] P. Song, W. B. Goh, W. Hutama, C.-W. Fu, and X. Liu, "A handle bar metaphor for virtual object manipulation with mid-air interaction," in *Proc. ACM Annu. Conf. Hum. Factors Comput. Syst. (CHI)*, Austin, TX, USA, 2012, pp. 1297–1306.
[9] D. Bassily, C. Georgoulas, J. Guettler, T. Linner, and T. Bock, "Intuitive and adaptive robotic arm manipulation using the leap motion controller," in *Proc. 41st Int. Symp. Robot.*, Munich, Germany, Jun. 2014, pp. 1–7.
[10] T. Yamashita, "Model and simulation for hand and leg," *J. Inst. TV Eng. Jpn.*, vol. 29, no. 11, pp. 865–869, Nov. 1975.
[11] M. Komori and H. Miyauchi, "Position operation method by leg motion and characteristics of leg motion during operation," *J. Jpn. Soc. Des. Eng.*, vol. 53, no. 7, pp. 511–526, Jul. 2018.
[12] J. Scott, D. Dearman, K. Yatani, and K. N. Truong, "Sensing foot gestures from the pocket," in *Proc. 23nd Annu. ACM Symp. User Interface Softw. Technol. (UIST)*, New York, NY, USA, 2010, pp. 199–208.
[13] E. Velloso, D. Schmidt, J. Alexander, H. Gellersen, and A. Bulling, "The feet in human–computer interaction: A survey of foot-based interaction," *ACM Comput. Surv.*, vol. 48, no. 2, p. 21, Nov. 2015.
[14] Y. Kume and A. Inoue, "Feasibility of feet-operated pointing device," *J. Inst. Image Inf. TV Eng.*, vol. 54, no. 6, pp. 871–874, Jun. 2000.
[15] T. Masuno, S. Saito, H. Takahashi, and M. Nakajima, "Waraji: Input device for controling movement through leg movement," *J. Inst. Image Inf. TV Eng.*, vol. 54, no. 6, pp. 833–839, Jun. 2000.
[16] T. Kawai, T. Kashiwagi, A. Nishikawa, Y. Nishizawa, and T. Nakamura, "Proposal of hands-free interface based on foot movement using images," *J. Jpn. Soc. Compt. Aided Srg.*, vol. 16, no. 3, pp. 192–203, Oct. 2014.
[17] N. Tanaka, T. Ueda, M. Nakao, T. Sato, K. Minato, M. Yoshida, and K. Kouketsu, "Evaluation of kinematic characteristics of the foot thumb for the development of a new input device," *Trans. Jpn. Soc. Med. Bio. Eng.*, vol. 43, no. 4, pp. 790–794, Dec. 2005.
[18] M. Ohkura, K. Sato, and H. Tachikawa, "Temporal Characteristics of Double-click Performed by Foot," *Jpn. J. Ergonom.*, vol. 36, pp. 596–597, Jun. 2000.
[19] Y. Huang, E. Burdet, L. Cao, P. T. Phan, A. M. H. Tiong, P. Zheng, and S. J. Phee, "Performance evaluation of a foot interface to operate a robot arm," *IEEE Robot. Autom. Lett.*, vol. 4, no. 4, pp. 3302–3309, Oct. 2019.
[20] J. Wentzel, D. J. Rea, J. E. Young, and E. Sharlin, "Shared presence and collaboration using a co-located humanoid robot," in *Proc. 3rd Int. Conf. Hum.-Agent Interact.*, New York, NY, USA, 2015, pp. 273–276.
[21] J. Ramos, A. Wang, and S. Kim, "A balance feedback human machine interface for humanoid teleoperation in dynamic tasks," in *Proc. IEEE/RSJ Int. Conf. Intell. Robots Syst. (IROS)*, Hamburg, Germany, Sep. 2015, pp. 4229–4235.

[22] E. Abdi, M. Bouri, E. Burdet, S. Himidan, and H. Bleuler, "Positioning the endoscope in laparoscopic surgery by foot: Influential factors on surgeons' performance in virtual trainer," in *Proc. 39th Annu. Int. Conf. IEEE Eng. Med. Biol. Soc. (EMBC)*, Seogwipo, South Korea, Jul. 2017, pp. 3944–3948.
[23] M. H. D. Y. Saraiji, T. Sasaki, K. Kunze, K. Minamizawa, and M. Inami, "MetaArms: Body remapping using feet-controlled artificial arms," in *Proc. 31st Annu. ACM Symp. User Interface Softw. Technol.*, Berlin, Germany, 2018, pp. 65–74.
[24] J. Hernandez, W. Amanhoud, A. Haget, H. Bleuler, A. Billard, and M. Bouri, "Four-arm manipulation via feet interfaces," in *Proc. AAAI-FSS AI-HRI*, Arlington, VA, USA, 2019.
[25] D. Ueno, H. Sugimoto, M. Nakashima, and R. Hamakawa, "Manipulating virtual object by three-dimensional user interface," in *Proc. Nat. Convers. IPSJ*, Nagoya, Japan, vol. 2012, pp. 295–296.
[26] J. S. Artal-Sevil and J. L. Montanes, "Development of a robotic arm and implementation of a control strategy for gesture recognition through leap motion device," in *Proc. Technol. Appl. Electron. Teaching (TAEE)*, Seville, Spain, Jun. 2016, pp. 1–9.
[27] Y. Matsui, T. Umezawa, and N. Osawa, "A method for adjusting position and orientation of virtual object with finger tracking," in *Proc. Nat. Convers. IPSJ*, Yokohama, Japan, 2016, pp. 241–242.
[28] I. Poupyrev, S. Weghorst, and S. Fels, "Non-isomorphic 3D rotational techniques," in *Proc. SIGCHI Conf. Hum. Factors Comput. Syst. (CHI)*, Hague, The Netherlands, 2000, pp. 540–547.
[29] B. Ionescu, V. Suse, C. Gadea, B. Solomon, D. Ionescu, S. Islam, and M. Cordea, "Using a NIR camera for car gesture control," *IEEE Latin Amer. Trans.*, vol. 12, no. 3, pp. 520–523, May 2014.
[30] J. L. Raheja, R. Shyam, U. Kumar, and P. B. Prasad, "Real-time robotic hand control using hand gestures," in *Proc. 2nd Int. Conf. Mach. Learn. Comput.*, Bengaluru, India, 2010, pp. 12–16.
[31] A. Sarkar, K. A. Patel, R. K. G. Ram, and G. K. Capoor, "Gesture control of drone using a motion controller," in *Proc. Int. Conf. Ind. Informat. Comput. Syst. (CIICS)*, Mar. 2016, pp. 1–5.
[32] A. Trenkle, M. Göhl, and K. Furmans, "Interpretation of pointing gestures for the gesture controlled transportation robot 'FiFi,'" in *Proc. Annu. IEEE Syst. Conf. (SysCon)*, Vancouver, BC, Canada, Apr. 2015, pp. 721–726.
[33] D.-S. Kwon, K. Young Woo, and H. Suck Cho, "Haptic control of the master hand controller for a microsurgical telerobot system," in *Proc. IEEE Int. Conf. Robot. Autom.*, Detroit, MI, USA, May 1999, pp. 1722–1727.
[34] S. Shirwalkar, A. Singh, K. Sharma, and N. Singh, "Telemanipulation of an industrial robotic arm using gesture recognition with kinect," in *Proc. Int. Conf. Control, Autom., Robot. Embedded Syst. (CARE)*, Jabalpur, India, Dec. 2013, pp. 1–6.
[35] R. Tadakuma, Y. Asahara, H. Kajimoto, N. Kawakami, and S. Tachi, "Development of anthropomorphic multi-D.O.F master-slave arm for mutual telexistence," *IEEE Trans. Vis. Comput. Graph.*, vol. 11, no. 6, pp. 626–636, Nov./Dec. 2005.
[36] C. A. Arango, J. R. Martinez, and V. Z. Perez, "Master-slave system using kinect and an industrial robot for teleoperations," in *Proc. Pan Amer. Health Care Exchanges (PAHCE)*, Medellin, Colombia, Apr. 2013, pp. 1–6.
[37] A. I. Kapandji, *Physiologie Articulaire II: Membre Inférieur*, E. S. Trans, Ed., 6th ed. Tokyo, Japan: Ishiyaku Publishers, 2009.
[38] K. Yonemoto, S. Ishigami, and T. Kondo, "The method guidelines for range of motion measurement," *Jpn. J. Rehabil. Med.*, vol. 32, no. 4, pp. 207–217, Apr. 1995.
[39] M. Komori, T. Terakawa, K. Matsutani, and I. Yasuda, "Posture operating method by foot posture change and characteristics of foot motion," *IEEE Access*, vol. 7, pp. 176266–176277, 2019.
[40] Y. Icaga, "Fuzzy evaluation of water quality classification," *Ecol. Indicators*, vol. 7, no. 3, pp. 710–718, Jul. 2007.
[41] S. Weon and J. Kim, "Learning achievement evaluation strategy using fuzzy membership function," in *Proc. 31st Annu. Frontiers Edu. Conf. Impact Eng. Sci. Educ. Conf.*, Reno, NV, USA, Oct. 2001, p. T3A-19.
[42] K. Hayashi and A. Otsubo, "Realization of PID control by fuzzy inference method and its application to hybrid control," *IEEJ Trans. Electron., Inf. Syst.*, vol. 118, no. 5, pp. 756–764, 1998.
[43] S. Jin, K. Watanabe, M. Nakamura, and T. Fukuda, "Nonlinear control for robot manipulators with artificial rubber muscles by using a fuzzy compensation," *J. Robot. Soc. Jpn.*, vol. 11, no. 5, pp. 737–744, Jul. 1993.
[44] D. A. Abbink and F. C. T. van der Helm, "Force perception measurements at the foot," in *Proc. IEEE Int. Conf. Syst., Man Cybern.*, Hague, The Netherlands, Oct. 2004, pp. 2525–2529.

MASAHARU KOMORI (Member, IEEE) received the B.E. degree in precision engineering from Kyoto University, in 1995, the M.E. degree from the Graduate School, Kyoto University, in 1997, and the Ph.D. degree in engineering from Kyoto University, in 2002.

In 2000, he became a Research Assistant at the Graduate School of Engineering, Kyoto University. In 2004, he became an Associate Professor at Kyoto University. In 2017, he became a Professor at Kyoto University, where he is currently with the Department of Mechanical Engineering and Science. His research interests include riding robotics, vehicles, robots, operation, transmission, gear, and measurement.

Prof. Komori is a Fellow of The Japan Society of Mechanical Engineers (JSME) and a member of The Robotics Society of Japan (RSJ), the Japan Society for Design Engineering (JSDE), and the Japan Society for Precision Engineering (JSPE). He was a recipient of the Young Scientists' Prize of the Commendation for Science and Technology by the Minister of Education, Culture, Sports, Science and Technology, in 2011, the WT Award, in 2013, three JSME Medals for Outstanding Paper, in 2009, 2013, and 2018, the JSME Medal for New Technology, in 2014, the JSME Young Engineers Award, in 2005, the Best Paper Award from JSDE, in 2012, the Eiji Mutoh Excellent Design Award, in 2012, the FA Foundation Paper Award, in 2014, and the Nagamori Award, in 2017. His article was selected as one of the best articles published in *Measurement Science and Technology*, in 2009.

TATSURO TERAKAWA received the B.E. degree in mechanical engineering from Kyoto University, Japan, in 2014, and the M.E. and Dr. Eng. degrees from the Department of Mechanical Engineering and Science, Graduate School of Engineering, Kyoto University, in 2016 and 2019, respectively.

Since 2019, he has been an Assistant Professor with the Department of Mechanical Engineering and Science, Kyoto University. His research in Kyoto University is focused on mechanisms and control of wheeled mobile robots, actuator mechanisms, and design.

Dr. Terakawa is a member of JSME and JSDE. He received the JSME Medal for Outstanding Paper, in 2018, the JSME Miura Award, in 2016, the JSDE Encouragement Award, in 2018, the IFToMM World Congress Best Application Paper Award, in 2019, the JSME MD&T Division Encouragement Presentation, in 2016, the FA Foundation Paper Award, in 2019, and the JSAE Graduate School Research Encouragement Awards, in 2016 and 2019.

IKKO YASUDA received the B.E. degree in mechanical engineering from Kyoto University, Japan, in 2018, and the M.E. degree from the Department of Mechanical Engineering and Science, Graduate School of Engineering, Kyoto University, in 2020.

His research in Kyoto University is on an operating method using foot motion.